Tenth International Congress
on Sound and Vibration
7-10 July 2003 • Stockholm, Sweden

ON THE "MODES" OF NON-HOMOGENEOUSLY DAMPED RODS HAVING TWO PARTS AND CARRYING A TIP MASS

H. Erol, M. Gürgöze
Istanbul Technical University, Faculty of Mechanical Engineering,
80191 Gümüşsuyu, Istanbul, Turkey.
E-Mail: erolha@itu.edu.tr

Abstract
This study is concerned with the determination of the eigenvalues and "eigenfunctions" of an axially vibrating, viscously damped elastic rod, carrying a tip mass and consisting of two parts having different physical parameters. The eigencharacteristics of the rod are determined via an original application of the separation of the variables method. The reliability of the method used is justified on a sample system, the eigenvalues of which are also calculated numerically by a finite element model.

INTRODUCTION

Recently, an interesting study [1] was published in which the eigencharacteristics of a continuous beam model with damping, are determined using the separation of variables approach. The beam considered has different stiffness, damping and mass properties in each of its two parts. Motivated by this publication, in [2], the present authors dealt with an axially vibrating rod consisting of two parts as a counterpart of that publication. Unlike the cited publication where overdamped and underdamped "modes" are investigated separately, both of them were handled simultaneously in [2], again via separation of variables approach. The present study is more general then the previous one because here, the rod is assumed to carry a tip mass as well.

THEORY

Let it be assumed that an axially vibrating rod carrying a tip mass M consists of two parts, one of length L_1 with axial rigidity E_1A_1, viscous damping coefficient c_1, and mass per unit length m_1, and the second of length L_2, with corresponding parameters E_2A_2, c_2 and m_2. These parameters are assumed to be constant along each rod segment, and contain contributions from the rod and any surrounding medium. Figure 1 shows the rod diagrammatically.

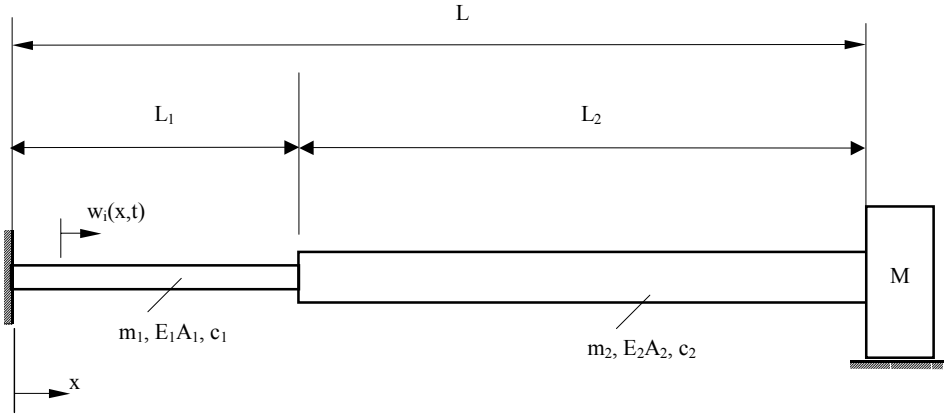

Figure 1. Axially vibrating elastic rod having two parts and carrying a tip mass.

Due to the presence of external viscous damping it is more appropriate to work with complex variables. It will be assumed that the axial displacements $w_i(x,t)$, (i = 1,2) of both parts of the rod are the real parts of the some complex quantities denoted as $z_i(x,t)$. Keeping in mind that actually, one is interested only in the real parts of the expressions below, the equations of motion of the rod can be written as

$$k_i z_i''(x,t) - m_i \ddot{z}_i(x,t) - c_i \dot{z}_i(x,t) = 0\,, \quad i = 1,2 \tag{1}$$

with $k_i = E_iA_i$, where E_iA_i denotes the axial rigidity of the ith portion and x is the axial position along the rod. Dots and primes denote partial derivatives with respect to time t and position coordinate x.

The corresponding boundary conditions are

$$\begin{gathered} z_1(0,t) = 0\,, \\ z_1(L_1,t) = z_2(L_1,t)\,, \quad k_1 z_1'(L_1,t) = k_2 z_2'(L_1,t)\,, \\ k_2 z_2'(L,t) + M\,\ddot{z}_2(L,t) = 0\,. \end{gathered} \tag{2}$$

Let it be assumed that

$$z_i(x,t) = Z_i(x)\,D_i(t)\,, \quad i = 1,2 \tag{3}$$

according to the separation of the variables approach, where both functions $Z_i(x)$ and $D_i(t)$ are complex functions in general. Substituting (3) into equations (1) gives

$$\frac{k_i}{m_i}\frac{Z_i''}{Z_i} = \frac{\ddot{D}_i + \left(\dfrac{c_i}{m_i}\right)\dot{D}_i}{D_i} := \kappa_i \tag{4}$$

where the κ_i are complex constants to be determined. Here, primes and dots denote derivatives with respect to position x and time t. To satisfy the second and third of the boundary conditions (2) these time functions must be equal, so that $D_1(t) = D_2(t) = D(t)$. Thus, the differential equations for $Z_i(x)$ may be written using equation (4) as follows:

$$Z_i''(x) - \frac{m_i}{k_i}\kappa_i Z_i(x) = 0, \quad i = 1,2. \tag{5}$$

The time function is assumed now as an exponential function

$$D(t) = e^{\lambda t} \tag{6}$$

where λ represents an eigenvalue of the system which is complex in general. With this D(t), the second equality in (4) gives

$$\kappa_i = \frac{c_i}{m_i}\lambda + \lambda^2, \quad i = 1,2. \tag{7}$$

with the abbreviation

$$\nu_i^2 = \frac{m_i}{k_i}\kappa_i, \quad i = 1,2 \tag{8}$$

the first equation in (4) can be written as

$$Z_i''(x) - \nu_i^2 Z_i(x) = 0, \quad i = 1,2. \tag{9}$$

The general solutions of the differential equations (9) can be expressed as

$$Z_i(x) = \overline{A}_i e^{\nu_i x} + \overline{B}_i e^{-\nu_i x}, \quad i = 1,2. \tag{10}$$

where $\overline{A}_i$ and $\overline{B}_i$ denote complex constants to be determined. In terms of the $Z_i(x)$, and with the aid of equation (6) the boundary conditions in equation (2) can be formulated as

$$Z_1(0) = 0,$$

$$Z_1(L_1) = Z_2(L_1), \quad k_1 Z_1'(L_1) = k_2 Z_2'(L_1),$$

$$k_2 Z_2'(L) + M\lambda^2 Z_2(L) = 0. \tag{11}$$

The substitution of the expressions (10) into (11) yields the following set of four homogeneous equations for the determination of $\overline{A}_i$ and $\overline{B}_i$:

$$\begin{bmatrix} 1 & 1 & 0 & 0 \\ 0 & 0 & \left(k_2\nu_2 + M\lambda^2\right)e^{\nu_2 L} & -\left(k_2\nu_2 - M\lambda^2\right)e^{-\nu_2 L} \\ e^{\nu_1 L_1} & e^{-\nu_1 L_1} & -e^{\nu_2 L_1} & -e^{-\nu_2 L_1} \\ k_1\nu_1 e^{\nu_1 L_1} & -k_1\nu_1 e^{-\nu_1 L_1} & -k_2\nu_2 e^{\nu_2 L_1} & k_2\nu_2 e^{-\nu_2 L_1} \end{bmatrix} \begin{bmatrix} \overline{A}_1 \\ \overline{B}_1 \\ \overline{A}_2 \\ \overline{B}_2 \end{bmatrix} = \begin{bmatrix} 0 \\ 0 \\ 0 \\ 0 \end{bmatrix}. \tag{12}$$

Let the matrix of the coefficients be denoted by **A**. For a nontrivial solution, the determinant of the matrix **A** should be zero:

$$\det\mathbf{A}(\nu_1, \nu_2) = \begin{vmatrix} 1 & 1 & 0 & 0 \\ 0 & 0 & \left(k_2\nu_2 + M\lambda^2\right)e^{\nu_2 L} & -\left(k_2\nu_2 - M\lambda^2\right)e^{-\nu_2 L} \\ e^{\nu_1 L_1} & e^{-\nu_1 L_1} & -e^{\nu_2 L_1} & -e^{-\nu_2 L_1} \\ k_1\nu_1 e^{\nu_1 L_1} & -k_1\nu_1 e^{-\nu_1 L_1} & -k_2\nu_2 e^{\nu_2 L_1} & k_2\nu_2 e^{-\nu_2 L_1} \end{vmatrix} = 0 \tag{13}$$

If in equation (13) the tip mass M goes to infinity, then the characteristic equation of the axially vibrating elastic rod fixed at both ends is obtained, which is given in reference [2]. Equating to zero the tip mass M yields the characteristic equation of the fixed-free rod.

Using the definitions given by (7) and (8), ν_1 and ν_2 can be expressed as functions of the eigenvalue λ

$$\nu_1(\lambda) = \pm\sqrt{\frac{m_1}{k_1}\left[\left(\frac{c_1}{m_1}\right)\lambda + \lambda^2\right]},\ \nu_2(\lambda) = \pm\sqrt{\frac{m_2}{k_2}\left[\left(\frac{c_2}{m_2}\right)\lambda + \lambda^2\right]}. \qquad (14)$$

Hence equation (13) becomes

$$\det \mathbf{A}(\nu_1(\lambda), \nu_2(\lambda)) = \det \mathbf{A}(\lambda) = 0 \qquad (15)$$

from which λ can be obtained, which is a complex number in general. Now via (14) ν_1 and ν_2 can be obtained. If these ν_1 and ν_2 are substituted into the coefficients matrix **A** in equation (12) the unknowns $\overline{A}_i$ and $\overline{B}_i$ (i = 1,2) can be determined up to an arbitrary constant. Hence, $Z_i(x)$ in equation (10) are obtained.

Returning to equation (3) considering equation (10) and introducing

$$\lambda = \lambda_{re} + j\lambda_{im}, \quad \nu_i = \nu_{i\,re} + j\nu_{i\,im},$$
$$\overline{A}_i = \overline{A}_{i\,re} + j\overline{A}_{i\,im}, \quad \overline{B}_i = \overline{B}_{i\,re} + j\overline{B}_{i\,im}, \quad (j = \sqrt{-1}) \qquad (16)$$

the axial displacements of the two rod portions $w_i(x,t)$ are determined, after lengthy calculations as

$$w_i(x,t) = \mathrm{Re}[z_i(x,t)] = e^{\lambda_{re}t}S_i(x)\cos\lambda_{im}t - e^{\lambda_{re}t}Q_i(x)\sin\lambda_{im}t \qquad (17)$$

where the following abbreviations are introduced

$$S_i(x) = e^{\nu_{i_{re}}x}\left(\overline{A}_{i_{re}}\cos\nu_{i_{im}}x - \overline{A}_{i_{im}}\sin\nu_{i_{im}}x\right) + e^{-\nu_{i_{re}}x}\left(\overline{B}_{i_{re}}\cos\nu_{i_{im}}x + \overline{B}_{i_{im}}\sin\nu_{i_{im}}x\right),$$
$$Q_i(x) = e^{\nu_{i_{re}}x}\left(\overline{A}_{i_{re}}\sin\nu_{i_{im}}x + \overline{A}_{i_{im}}\cos\nu_{i_{im}}x\right) + e^{-\nu_{i_{re}}x}\left(\overline{B}_{i_{im}}\cos\nu_{i_{im}}x - \overline{B}_{i_{re}}\sin\nu_{i_{im}}x\right). \qquad (18)$$

The expressions of the axial displacements can be put in a more compact form, as

$$w_i(x,t) = e^{\lambda_{re}t}C_i(x)\cos(\lambda_{im}t - \varepsilon_i(x)) \qquad (19)$$

with

$$C_i(x) = \sqrt{S_i^2(x) + Q_i^2(x)}, \quad \tan\varepsilon_i(x) = -\frac{Q_i(x)}{S_i(x)} \qquad (20)$$

$w_i(x,t)$, i = 1,2 determine the axial displacement distribution over the length of the viscously damped rod carrying a tip mass when it vibrates at an eigenvalue λ. Due to the apparent presence of a phase which is a function of the position coordinate x, the authors preferred to use the expression "mode" or "eigenfunction" as seldom as possible. Whenever necessary, those words were used in quotation marks.

NUMERICAL EVALUATIONS

This section is devoted to the numerical evaluation of the expressions obtained. The computation will be demonstrated using a rod with the parameters given in Table 1. The eigenvalues and "eigenfunctions" are computed using the procedure outlined above, and also using a finite element model for comparison. The finite element model has 45 elements of equal length, giving a total of 90 degrees of freedom.

Table 1. Physical parameters for the numerical example.

	Case 1		**Case2**	
M = 50 kg	**Rod 1**	**Rod 2**	**Rod 1**	**Rod 2**
L_i [m]	1	2	1	2
m_i [kg/m]	10	20	10	20
c_i [kg/ms]	500	500	1000	0
E_iA_i [N]	100	200	100	200

Two cases are considered: In the first case, it is assumed that both parts of the rod are subjected to the same external viscous damping action of $c_1 = c_2 = 500$ kg/ms. In case 2, the first part of the rod is subjected to the damping action of $c_1 = 1000$ kg/ms whereas the second part is undamped.

Table 2 gives the "first" six eigenvalues of the system for both cases. It is seen that both cases lead to both overdamped and underdamped modes. The numerical values in the first columns of each case represent the results of the present methodology whereas those of the second columns are results of a finite element model.

The upper part of Figure 2 shows for case 1 the three dimensional plots of $w_i(x,t)$ for the first three overdamped eigenvalues. In the lower part, as representatives of the damped "eigenbehavior", those curves are plotted which result from the intersection of this "eigensurfaces" above with the $t = 0$ plane. These curves could be viewed as "eigenfunctions". It is seen from Figure 2 that the amplitudes of the intersection curves corresponding to increasing t values decrease in accordance with the damped character of the system.

As in Figure 2, the upper part of Figure 3 shows for case 1, the $w_i(x,t)$ surfaces for the "first" three underdamped eigenvalues. The lower part gives the "eigenfunctions" in the sense explained above.

The Figures 4 and 5 are concerned with case 2 in which the second part of the rod is undamped, whereas the first part is damped strongly. As in Figures 2 and 3, the upper parts of Figures 4 and 5 reflect the $w_i(x,t)$ plots of the first three overdamped and underdamped eigenvalues, respectively. The lower parts give the corresponding "eigenfunctions".

The comparison of the surfaces in Figures 2 and 4 reveals that the surfaces in Figure 4 tend to level at zero more rapidly than those in Figure 2, which is due to the fact that the absolute values of the eigenvalues corresponding to Figure 4 are much higher than those of Figure 2. The comparison of the surfaces in Figures 3 and 5 shows that the situation is reversed this time.

Table 2. "lower" eigenvalues of the numerical example.

Case 1	
Continuous Model	**Finite Element Model**
-0.06802	-0.06802
-0.87203	-0.87203
-2.60611	-2.60619
-1.78869 ± 2.83203i	-1.78869 ± 2.83203i
-14.58138 ± 4.33863i	-14.57964 ± 4.34106i
-14.20533 ± 12.74677i	-14.12624 ± 12.71483i

Case 2	
Continuous Model	**Finite Element Model**
-0.25891	-0.25891
-2.60406	-2.60442
-7.58911	-7.59736
-0.13054 ± 1.10190i	-0.13054 ± 1.10190i
-0.41502 ± 4.84037i	-0.41506 ± 4.84023i
-0.58731 ± 9.40117i	-0.58748 ± 9.40037i

On the other hand, as in reference [1], in accordance with the fact that in case 2 the first part of the rod is damped strongly whereas the second part is not, one observes that the majority of the displacements in the "lower" underdamped "modes" is local to the undamped, namely second part of the rod.

The "eigencurves" corresponding to lower overdamped eigenvalues in cases 1 and 2 behave similarly, regarding the number of the nodes, which can be seen from comparison of Figures 2 and 4. On the contrary, "eigencurves" corresponding to lower underdamped "eigenvalues" in both cases behave differently. The number of nodes in case 2 is much less than that in case 1, as can be seen from the comparison of Figures 3 and 5.

CONCLUSIONS

This study is concerned with the establishment of a method to compute the eigenvalues and "eigenfunctions" of a continuous, viscously damped rod, carrying a tip mass and consisting of two parts having different physical parameters.

Both the overdamped and the underdamped eigenvalues and corresponding "eigenfunctions" have been computed for two different sets of damping parameters. For high damping the lower underdamped "modes" seem to be local to the undamped part of the rod.

REFERENCES

1. Friswell, M.I., and Lees, A.W., 2001, "The modes of non-homogeneously damped beams", Journal of Sound and Vibration, **242**, pp. 355-361.
2. Gürgöze, M., and Erol, H., 2003, "On the "modes" of non-homogeneously damped rods consisting of two parts", Journal of Sound and Vibration, **260**, pp. 355-361.

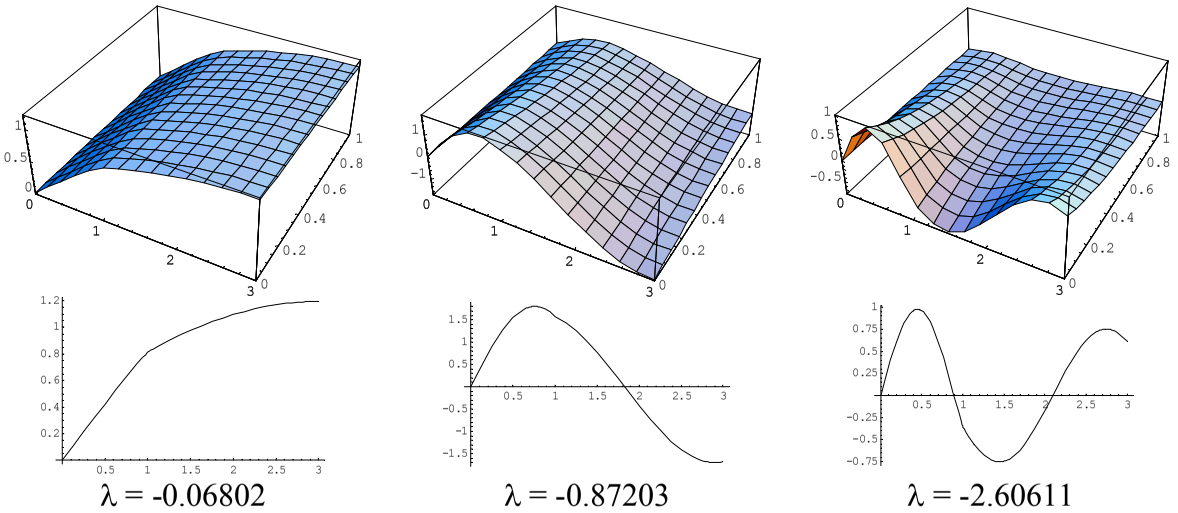

Figure 2. Plots of $w_i(x,t)$–surfaces and their intersection curves with t=0 plane, corresponding to the first three overdamped eigenvalues for case 1.

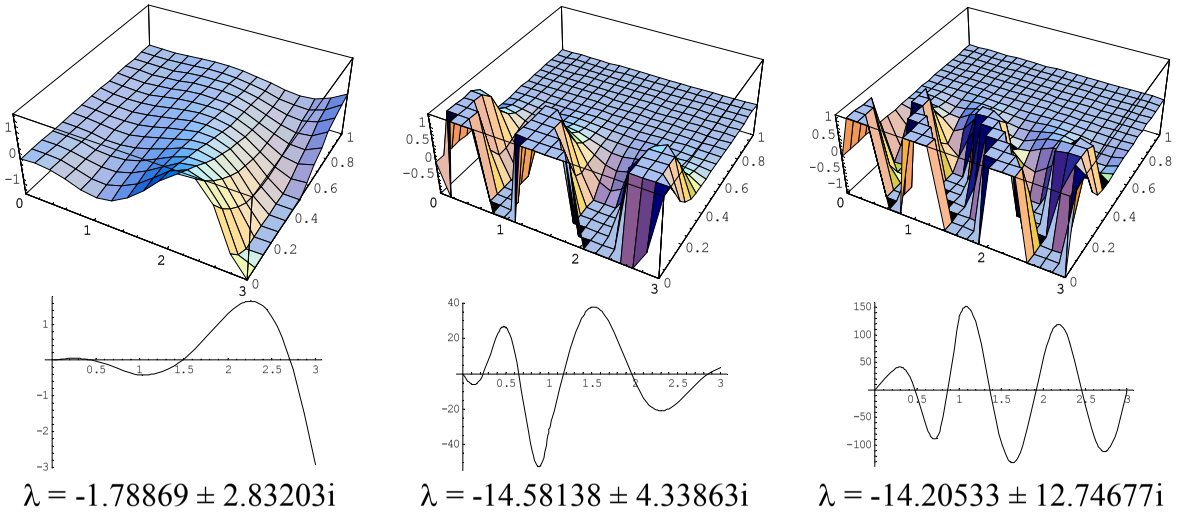

Figure 3. Plots of $w_i(x,t)$–surfaces and their intersection curves with t=0 plane, corresponding to the first three underdamped eigenvalues for case 1.

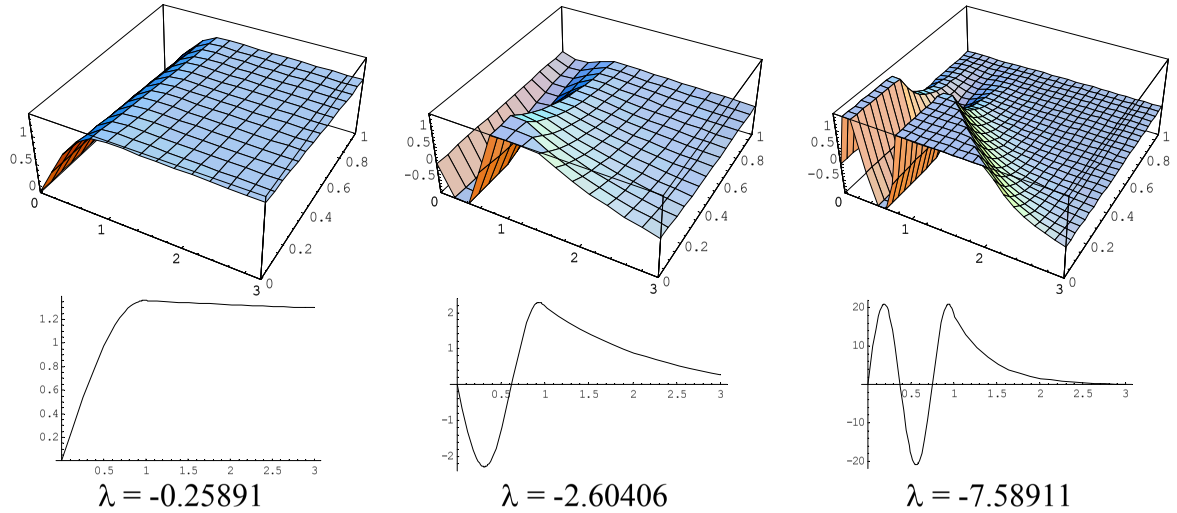

Figure 4. Plots of $w_i(x,t)$–surfaces and their intersection curves with t=0 plane, corresponding to the first three overdamped eigenvalues for case 2.

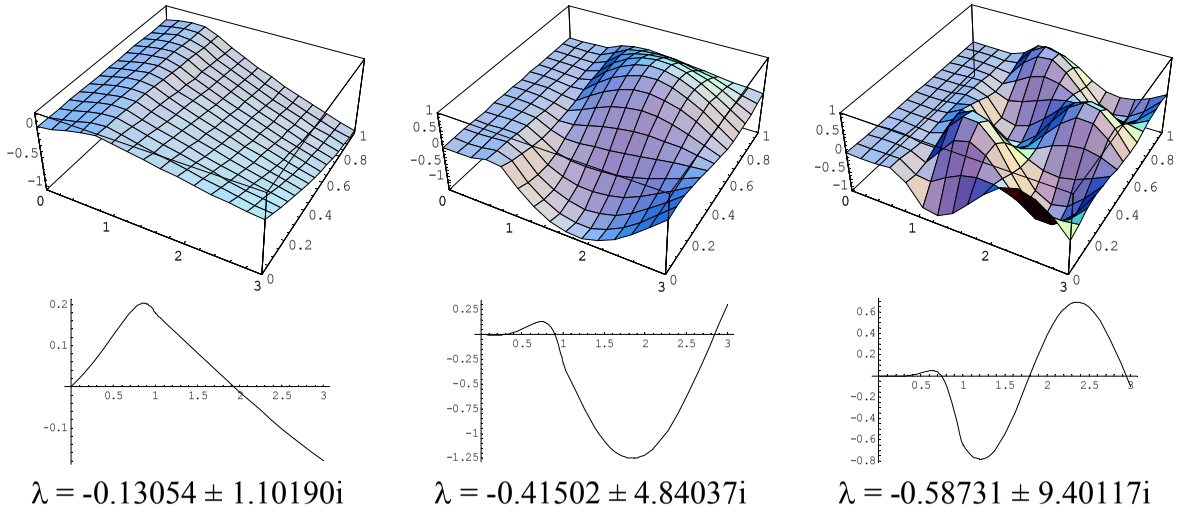

Figure 5. Plots of $w_i(x,t)$–surfaces and their intersection curves with t=0 plane, corresponding to the first three underdamped eigenvalues for case 2.